Stranding Moso and Guadua Bamboo. Part II. Strand Surface Roughness and Classification

Kate E. Semple, Polo K. Zhang, and Gregory D. Smith*

In this study OSB strands produced by a CAE 6/36 disk flaker from re-saturated moso and guadua bamboo tissue were classified by surface quality and compared with industrial aspen OSB strands. Strands were first classified into three groups based on surface appearance and texture. The topographic features that characterize the surface were then measured using a laser surface profiler to give two surface roughness indicators; average roughness (Ra) and average maximum roughness (Rz). Guadua strand surface quality was extremely poor compared to moso due to its very large, dense vascular bundles. Ra and Rz values for many bamboo strands, particularly guadua, exceeded the typical diameter of resin droplets dispensed during industrial OSB blending, meaning that excessive roughness could compromise bonding efficiency in bamboo OSB.

*Contact information: Department of Wood Science-Composites Group, University of British Columbia, 2900-2424 Main Mall, Vancouver, BC, Canada, V6T 1Z4; *Corresponding author: greg.smith@ubc.ca*

INTRODUCTION

In Part II of this series on stranding moso (*Phyllostachys pubescens* Mazel) and guadua (*Guadua angistifolia* Kunth) bamboo, the surface quality and roughness indices of strands were assessed. Part I (Semple *et al.* 2015a) covered strand production using a CAE 6/36 laboratory disk flaker, pole characteristics affecting strand size and quality, and compared frequency distributions for strand width and thickness against a standard industrial aspen OSB mill furnish. To minimize the amount (and cost) of resin required to manufacture OSB, strands are spot-welded together by very small, dispersed droplets of resin (Kamke *et al.* 1996; Smith 2003a,b). There is very little information available on the measured surface roughness of OSB strands, and none for bamboo strands. Information on how it may affect the efficiency of bonding of small droplet arrays deposited during the resin atomization and blending process is also lacking. The very rough surfaces of many of the bamboo strands observed in Part I may be different to and outside the range of surface roughness found in standard OSB furnish, and potentially reduce the bonding efficiency of very small adhesive droplet arrays.

The surface of a machined piece of wood (such as a sliced OSB strand) is a complex function of three levels of texture (Marian *et al.* 1958): the woods' own anatomical features (*e.g.*, vessels), intentional machining features (*e.g.*, smooth slicing by a planer or roughening from sand paper), and errors of form (*e.g.*, material distortion and variability in tooling and machine performance that produces 'background' effects such as waviness or deep cracks). Notwithstanding errors of form, the induced surface roughness of wood adherends has significant effects on adhesive wettability and final adhesive bond strength

and fracture toughness (Collett 1972; Ebewele *et al.* 1980; Nussbaum and Sterley 2002). To bond wood surfaces, specialized liquid adhesives have been developed that allow wetting and conformation with the surface, but limit seepage into the substrate and its resultant starvation of the glueline. Therefore surface characterization of wood and OSB strands commonly includes assessment of surface energy, with measurement of contact angles in relation to adhesive wettability (Shupe *et al.* 1998; Maldas and Kamdem 1999; Shi and Gardner 2001; Nussbaum and Sterley 2002).

One of the biggest problems with defining wood surface roughness in relation to adhesion is the porous and permeable nature of the wood, giving it 'internal roughness' that is not picked up by stylus tracings (Ebewele *et al.* 1980). Some drawbacks of stylus tracings include slow measurement speed, surface damage, catching of the stylus in holes or deep fissures, 2-dimensional sampling, results being influenced by environmental vibrations, and stylus and arm variables (Devoe *et al.* 1992; Hu and Afzal 2005). Today, stylus tracings have largely been replaced by non-contact methods of laser displacement sensing of the surface to map the surface topography (Lundberg and Porankiewicz 1995; Sandak and Tanaka 2003; Sandak *et al.* 2004; Hu and Afzal 2005). A commercially available non-contact laser profiling system was used in this study, due to occasional deeply fissured surfaces, and detached tissue on bamboo strands susceptible to dislodgement by a stylus.

The objective of this study was to measure the surface roughness indices (average roughness, *Ra*, and maximum roughness, *Rz* of bamboo strands classified by feel as 'smooth' or 'rough' and compare these indices with those measured on 'smooth' and 'rough' industrial OSB strands produced from aspen (*Populus tremuloides* Michx). The results are compared to and discussed in relation to the known size of resin droplets administered during OSB furnish blending.

EXPERIMENTAL

Assessment of strand surface quality was done in two ways. First, a qualitative classification using a combination of visual and tactile assessments of each measured strand from Part I was made as to whether each strand fell into one of three surface roughness groupings: (1) rough on both sides, (2) smooth on one side and rough on the other, or (3) smooth on both sides. Tactile assessment of surface roughness can be subjective, particularly if there are several categories, and the boundaries between categories are indistinct. For this reason, the number of categories was restricted to three, with most sampled strands easily classified into one of the three.

Second, a laser surface profiler from LaserScan LT (Solaris, San Francisco, USA), fitted with a Keyence K2000 Series LK-031 sensor head, was used to measure the topographic features, *i.e.*, the height and depth of the ridges and valleys running parallel to the length of the strand. This was done to quantitatively characterize surfaces assessed subjectively by touch as either 'rough' or 'smooth' in each type of sliced tissue (aspen, moso, and guadua). Surface profile data were mapped and analyzed using Solar Map Universal 3.2 software. Six specimens, each of seven types of surface, were scanned for a total of 42 scans. The seven surface types were (1) aspen 'smooth', (2) aspen 'rough', (3) moso 'smooth', (4) moso 'rough', (5) guadua 'smooth', (6) guadua 'rough', and (7) a 'smooth' reference surface of sliced moso bamboo veneer. This cabinet-quality veneer is produced in China by pre-softening large laminated billets and using a large sharpened

wedge blade to slice thin veneer sheets measuring 2400-mm × 1200-mm × 0.6-mm in thickness. The veneer is kept intact by a layer of high tear strength paper adhered to the back.

Each sampled strand was first clipped to a length of 60 mm and affixed to a small 10-mm-thick aluminum block using large bulldog clips to keep the scanned surface flat. Each scan was 10 mm by 10 mm in area, with a measurement increment of 1 μm in the *x*-direction (*i.e.*, across the grain or 'lay', in machining terms). The average roughness profile was compiled from a total of 50 cross-grain scans taken at increments of 200 μm along the grain (*y*-direction). The process took approximately 20 minutes per scan. The presence of localized flaws or tiny holes in the specimen gave a miss-read, and greatly distorted the true primary surface roughness profile. These were manually identified and removed from the series before compiling the average roughness profile for a specimen. Specimens with a crack running much of, or the entire, length of the sampling zone were unable to be reliably measured and were eliminated. As per the standard procedures for measuring and deriving surface roughness covered in ISO 4287 (2000) and ISO 16610 (2011), the primary 10 mm profile was truncated by 1 mm at both ends, and a basic Gaussian regression filter was applied to give the average roughness profile. The Gaussian filter removes the confounding errors of form in the surface, such as slope or waviness. From the average roughness profile, the following indices were calculated: average roughness (R_a) and average maximum roughness (R_z) (Eqs. 1 and 2). R_a is the arithmetic average of all the absolute values for peak height and valley depth from center line, and R_z is the average of the five highest values in magnitude peak height and valley depths,

$$R_a = \frac{1}{n}\sum_{i=1}^{n}|y_i| \tag{1}$$

$$R_z = \frac{1}{5}\sum_{i=1}^{5}R_{pi} - R_{vi} \tag{2}$$

and R_{pi} and R_{vi} are the ith highest peak and lowest valley, respectively.

A DX100 Olympus Digital Light Reflection Microscope (5x magnification) was used to examine the sliced transverse cross-sections through the culm wall of moso and Guadua tissue. This was to provide a visual comparison of the morphology of the vascular bundles likely affecting the surface quality of the sliced strands.

RESULTS AND DISCUSSION

Qualitative Classification into Surface Roughness Classes and Surface Macro Features

Cursory examination of both industrial aspen mill strands and bamboo strands suggested considerable visual and tactile variation in the surface roughness of strands. The surface quality of wood products is still often assessed by feel (tactile) judgment, but due to the complexity and variability of the material no universally accepted standard parameter for characterizing and comparing the roughness of wood surfaces has ever been developed (Fujiwara *et al*. 2004). The macroscopic visual appearance of strand surfaces of moso, guadua, and aspen mill strands subjectively assessed 'rough' and 'smooth' to touch is shown in Figure 1a to c. Figure 1d shows the surface condition at the site of node tissue in

the culm wall. Note the much wider zone of node tissue in the guadua strands. Slicing through the site of the embedded node tissue in the culm wall of guadua resulted in a very uneven, and in many cases broken up, surface.
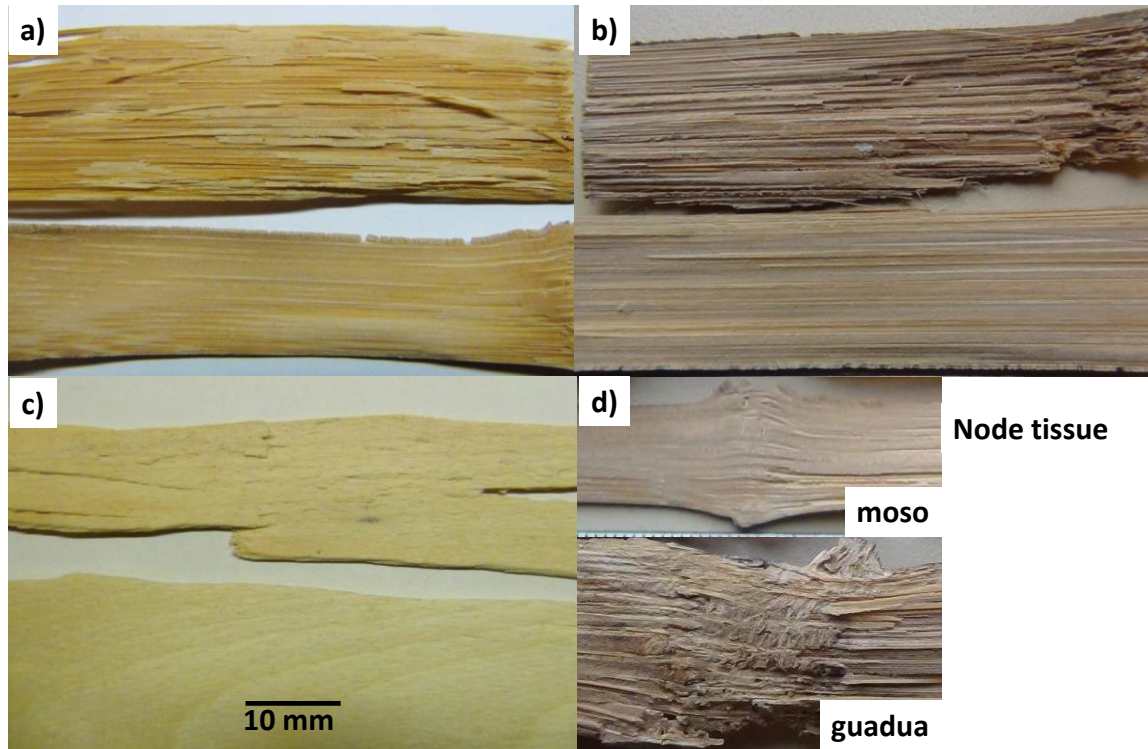
Fig. 1. Surface appearance of: (a) moso, (b) guadua, (c) aspen mill strands. The top strand surface in the images was classified as 'rough', and the bottom strand surface was classified as 'smooth'. (d) shows the appearance of the sliced node tissue in moso and guadua.

The proportions of moso and guadua strands falling into each of the three surface quality categories, stranded using the same flaker operating parameters, are given in Table 1. The majority (60%) of industrial aspen strands could be classified as 'smooth' on both sides, and 10% were classified as 'rough' on both sides. Experiments (Semple *et al.* 2014) in adjusting tissue MC and flaker operating parameters to optimize the thickness distribution and quality of strands from moso bamboo found that strand surface quality for moso was very sensitive to tissue moisture content, knife protrusion settings, material feed rates, and whether the pieces were stranded horizontally or vertically, *i.e.*, slicing across or along the grain, respectively. Full tissue saturation above 130% MC, low knife protrusion settings, slower feed rates, and stranding parallel to the fiber direction are all necessary to maximize the proportion of 'smooth-both-sides' strands.

Table 1. Percentage of Strands in Each Surface Category, *n* = 250

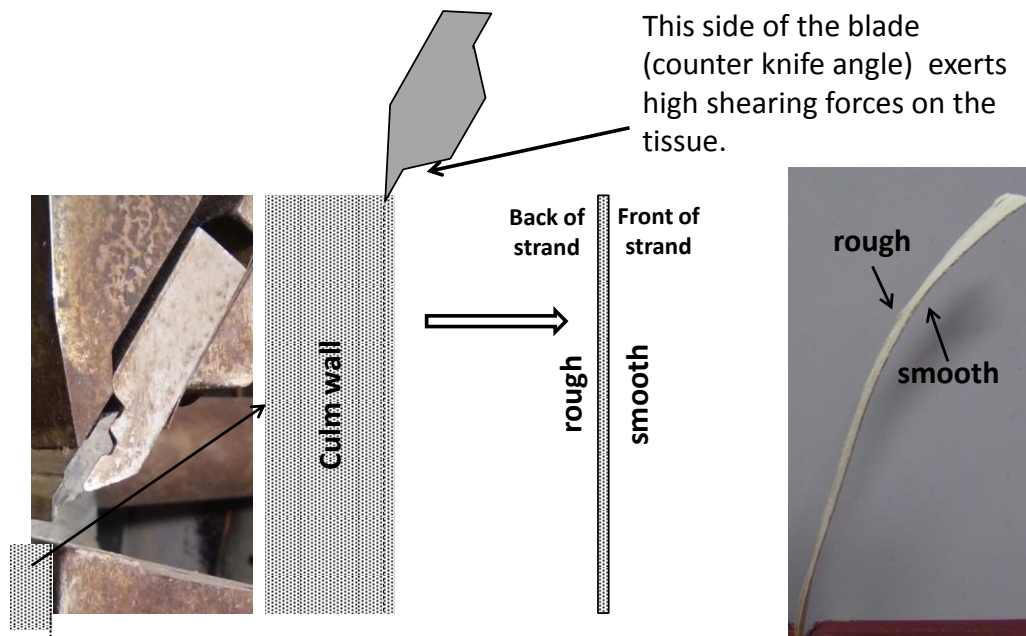| Material	Rough both sides	Smooth-Rough[*]	Smooth both sides
aspen	11	30	59
moso	49	25	26
guadua	65	30	5

[*]Smooth-Rough: one surface smooth, the other rough

Despite these efforts, no more than about a quarter of the bulk moso strands could be classified as 'smooth' on both sides. Another quarter of the bulk moso strands were distinctly smooth on one side and rough on the other. The rough surface of these moso strands is characterized by the presence of very thin and flat strips of parenchyma tissue that has sheared away from the bulk strand tissue, as seen in Fig. 1a and close-up in Fig. 2a.

a)

b)

2 mm   **400 µm**
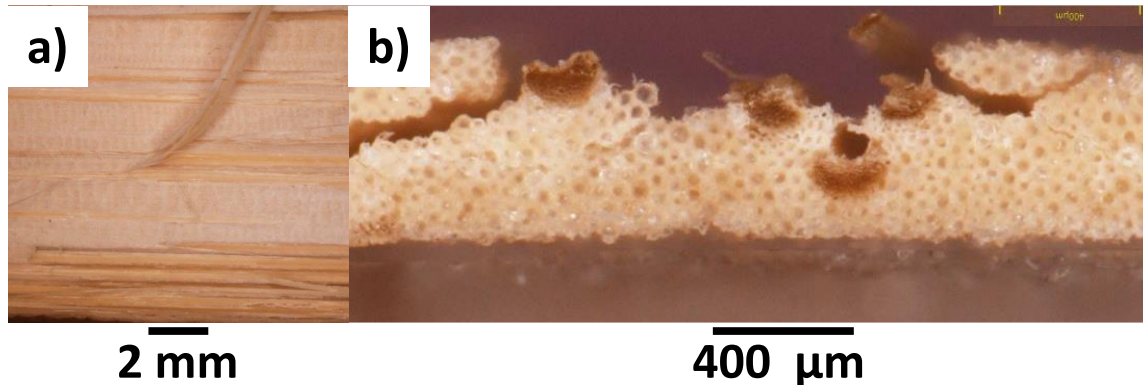
Fig. 2. Light microscopy image of the (a) top surface, and (b) transverse section through a sliced strand showing the detached parenchyma tissue dislodged from the back of the strand

The observed generation of rough surfaces is believed to be due to tensile stress and shearing forces acting on the backs of strands. This may be caused by the angled back of the cutting blade. The counter knife angle is designed to force sliced wood veneers to break up along the grain into narrower pieces to ensure most strands end up between about 25 and 50 mm in width (Maietta *et al.* 2011). A higher angle is used for denser, stronger woods. A schematic diagram of the slicing action is shown in Fig. 3.


This side of the blade (counter knife angle) exerts high shearing forces on the tissue.

Culm wall

Back of strand   Front of strand

rough   smooth

rough

smooth

Fig. 3. Schematic diagram explaining the phenomenon of 'sidedness' in bamboo strands produced on a disk flaker

bioresources.com

Three factors that were unable to be changed during stranding were the knife profile, counter knife angle, and the need to boil the pieces to re-saturate them prior to stranding. According to De Vallance *et al.* (2012), two adjustable process variables — MC and knife angle, directly impinge on the strand size and surface quality of 'difficult-to-strand' hardwoods like red oak. Knife angle critically affects the surface quality of veneer sliced from blocks (Spelter 1991). De Vallance *et al.* (2012) were able to make significant improvements to the size and quality of red oak strands by reducing knife speed down from current industrial flaker settings and using blades with a lower counter knife angle, thus placing less fracture stress on the material. Here, the bamboo tissue was saturated to its maximum capacity to ensure that tissue dryness was not a limiting factor, but it was not possible to adjust the counter knife angle. It is therefore possible that further improvements in the quality of both guadua and moso strands could be had by reducing or eliminating the counter knife angle, as well as other adjustable parameters such as cutting speed. The profiled counter knife is also unnecessary since the width of bamboo strands is already constrained by the limited culm wall thickness.

Strand quality in guadua was markedly lower than that of moso, despite using the same stranding parameters used to produce the best outcome for moso. From Table 1 only 5% of the sampled bulk guadua strands could be classified as 'smooth' on both sides. The majority of guadua strands (65%) were both visually and tactilely 'rough' on both surfaces. Many of these were split apart, as seen in Fig. 2b (top strand), rather than sliced cleanly, as seen in Fig. 2b (bottom strand). The appearance of the transverse surface across the grain of the culm wall of moso and guadua is shown in Fig. 4.
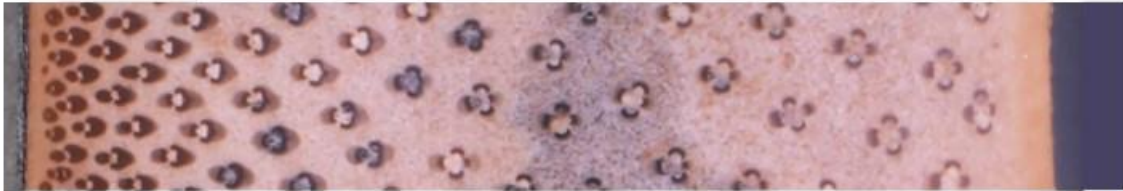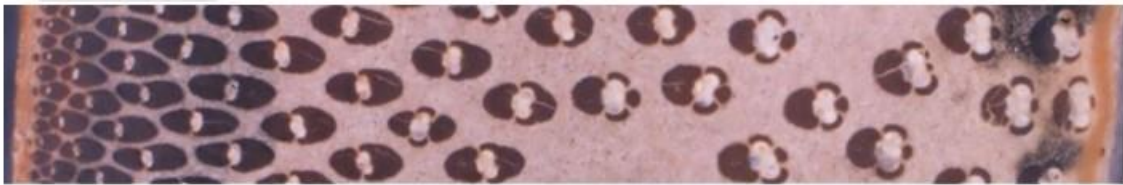
Fig. 4. Cross section through the culm wall of moso and guadua (2x)

The very large and solid vascular bundles present in guadua give it higher average density and far superior flexural stiffness than moso. From Part I, the average basic density of the stranded guadua and moso culm tissue was 533 kg/m^3 and 447 kg/m^3, respectively. Comparative tests on the two species by De Vos (2010) showed guadua to be 75% higher in MOE (14 GPa) of internode tissue than moso, but only slightly higher in MOR (130 MPa compared to 115 MPa for moso). Interestingly, De Vos (2010) found guadua to be less than half the Janka hardness of moso (2500 N compared to almost 6000 N for moso

internode tissues). Despite this apparent difference in hardness, guadua was still far more problematic to strand than moso, likely because of its greater average density and the more extreme differences in density and hardness of the two main culm wall tissue components: the fiber bundles, and the surrounding parenchyma ground tissue. Many of the guadua strands tended to split apart rather than slice cleanly, producing a rough surface with lots of raised ridges that correspond to the separation of the very large and solid fiber bundles (also known as vascular bundles) from the much softer and weaker parenchyma tissue. The largest of the vascular bundles of guadua were around 1.1 mm high and 0.5 mm wide, similar to those observed and measured by Aijazi (2013) in scanning electron microscopy images though the culm wall cross section of guadua. These very large, closely spaced fiber bundles in guadua tissue are in contrast with the much smaller and more discrete vascular bundles of moso tissue of the transverse section of the culm wall. In contrast, moso vascular bundles are approximately 40 µm high and 300 µm wide (Dixon and Gibson 2014). In the moso tissue sampled, many of the fiber sheathes (there are four in a whole fiber bundle) appeared not to be fully solidified, as shown by the light brown zones. This suggests that the fibers may have not yet reached their full maturity and density, and helps explain the much lower basic density of the moso (447 kg/m^3). After 1 year, bamboo fibers are hollow and thin walled, and over several subsequent years the fiber walls thicken and the cells solidify almost completely, leaving minimal lumen space (Leise and Weiner 1996).

While the volume fraction of fibers in the culm wall of bamboo is strongly gradational across the culm wall, the average volume fraction for guadua ranges from about 42% to 49% (Estrada *et al.* 2014). Fiber volume fraction for moso is on average around 40% (Osorio *et al.* 2010), and ranges from 15 to 20% in the inner wall to 60-65% at the outer wall (Amada *et al.* 1997). Guadua fibers are not only more voluminous compared to moso, but they are also very dense at 1440 kg/m^3 (Trujillo *et al.* 2010). The fibers are extremely tough and strong with a reported tensile strength and elastic modulus (tensile) of chemically extracted fibers of 234 MPa and 20.6 GPa (Ramirez *et al.* 2012), and for fibers extracted using optimized mechanical extraction, 800 MPa and 43 GPa, respectively; these values are comparable to those of glass fibers (Van Vuure *et al.* 2009; Trujillo *et al.* 2010). The parenchyma cells of the ground tissue surrounding the vascular bundles are very short and blocky with thin walls (Leise and Grosser 1972; Leise 1998), and the tissue density is just 330 kg/m^3 (Dixon and Gibson 2014). Its strength is only a tenth of that of the vascular bundles themselves (Amada *et al.* 1997). Unless the blade is very sharp and slices cleanly through the fiber bundles longitudinally, the shearing force exerted along the culm wall will simply rupture the parenchyma tissue surrounding the fibers, leaving them exposed on the surfaces of strands, giving the kind of surface seen in Fig. 2b (top strand).

In the stranded culm materials the frequency of nodes in the culm was less for guadua (3.3 nodes per m) than moso (3.8), but the node plates and embedded node tissue in guadua was over twice as thick (Semple *et al.* 2015a). Note in Fig. 2d the much greater damage to the surface caused by slicing through embedded node tissue in guadua compared with moso. Previous research (De Vos 2010) has noted the very poor planed surface quality of solid guadua tissue, especially at the nodes. In the node zone of the culm wall the anatomy of the vascular bundles changes considerably, becoming extensively branched, intertwined, and interconnected by repeated anastomoses (Grosser and Leise 1971). Fiber length is also shortest at the nodes, leading to greater tissue weakness (Leise and Grosser 1972; Shao *et al.* 2010). Sampling of the noded strands from guadua found up to 45% of

the bulk strands broken into two shorter pieces. Slicing this tissue would be akin to trying to slice through a knot of very thick rope.

The only known previous attempt to convert guadua tissue to strands was conducted by Dagilis (1999), similarly using a disk flaker. The author found that wafer quality was so poor as to preclude the fabrication of waferboards (the precursor to OSB), but did not elaborate on any wafer quality parameters such as breakage or surface characteristics. Short of simply cross cutting guadua culms into shorter rounds and discarding the node sections, there appears to be currently no practical way of removing the node plates. Since docking culms into short lengths is impractical and wasteful, a purpose-designed corer with a hardened steel or diamond-tipped tooling head would be a useful development for the guadua processing industry. The nodes are also largest and most numerous in the bottom portion of each whole culm, so one relatively simple strategy for minimizing the effects of nodes on OSB boards may be to separate the lower portion of each culm and only use the strands from these in the core layers of boards where consistency of strand length and strength properties is not as critical.

Surface Roughness Profiles

Average R_a and R_z values, and coefficient of variation (CV) for the six specimens from each of seven surface types are given in Table 2. A visual example of the raw surface roughness profiles (Fig. 5) and the typical 3-D topographic map constructed for a surface (Fig. 6) is shown for the 'smooth' and 'rough' surface of guadua strands. For the purpose of this study, a characteristic average roughness index was measured to characterize the two subjective tactile roughness groupings 'rough' and 'smooth.

Table 2. R_a and R_z Values for Different Surface Types ($N = 6$)

|	Ra (µm)	CV (%)	Rz (µm)	CV (%)
aspen smooth	10.11	10.31	57.98	10.66
aspen rough	17.37	15.91	113.83	38.04
moso smooth	7.70	7.60	43.97	7.89
moso rough	20.87	20.18	115.43	37.02
moso veneer	7.19	10.18	37.63	8.54
guadua smooth	10.70	26.61	57.33	20.27
guadua rough	23.38	16.61	115.22	14.91

The smoothest of the 'smooth' to touch surfaces was the fine sliced moso cabinet-makers veneer, $R_a = 7.19$ µm, followed by the 'smooth' moso strands, $R_a = 7.70$ µm. Corresponding R_z values for these two surfaces were 37.63 µm and 43.97 µm, respectively. Interestingly, the industrial aspen strands classified by touch as 'smooth' were similar in measured surface characteristics to the guadua strands classified as 'smooth'; $R_a = 10.11$ µm and 10.70 µm, and $R_z = 57.98$ µm and 57.33 µm, respectively. The strands from the three tissue types classified by touch as 'rough' were more variable in their measured surface characteristics. The roughest surfaces were found on guadua strands, $R_a = 23.38$ µm. It is interesting to note that all the strand surfaces subjectively classified by feel as 'rough' were remarkably similar in the measured topographic feature that makes them noticeably rough to feel, *i.e.*, the average vertical distance of the five highest and lowest peaks and valleys of the surface, represented by R_z. Average R_z values are 113.83 µm, 115.43 µm, and 115.22 µm for the 'rough' to touch aspen, moso, and guadua strands, respectively. However, note also the very high CV values in Table 2, especially for R_z of

'rough' surfaces indicating the large variation in measured roughness within the two groups.
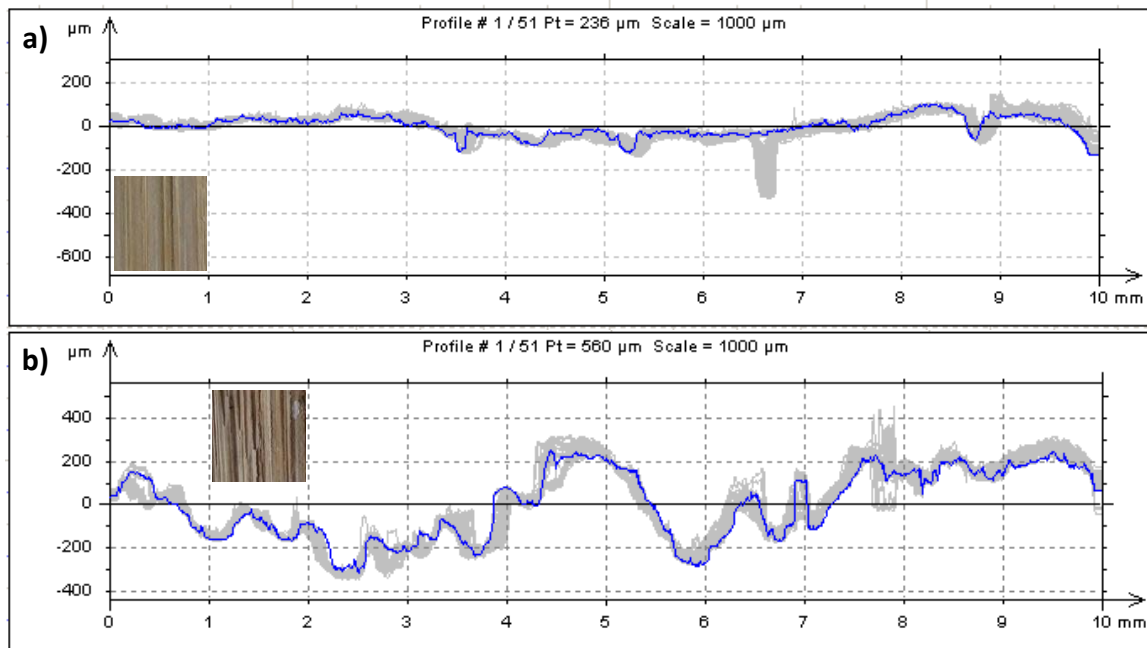
Fig. 5. Typical raw surface roughness profiles for guadua: (a) 'smooth' surface, and (b) 'rough' surface
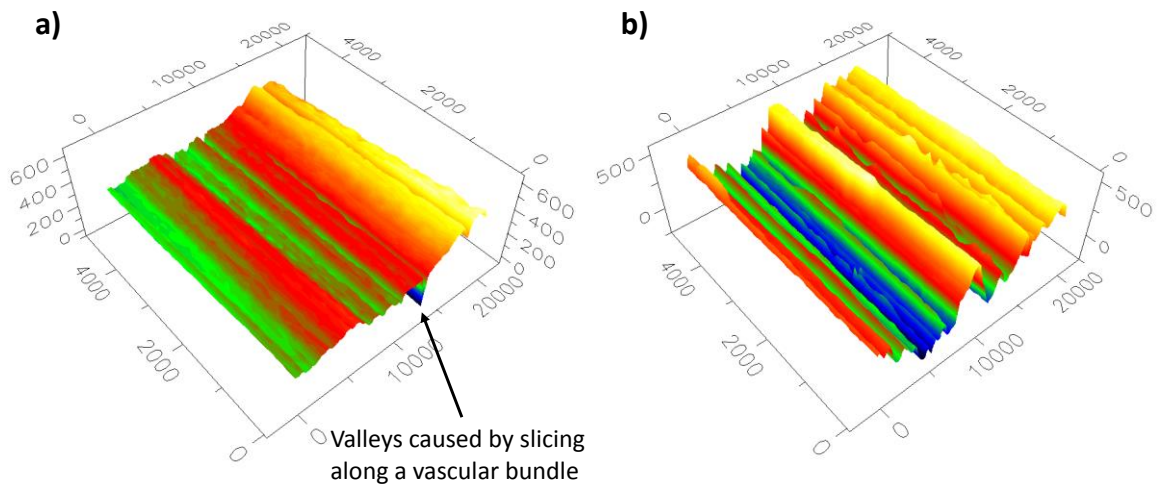
Fig. 6. Examples of topographic surface maps constructed from the raw profiles, for guadua strands: (a) 'smooth' surface, and (b) 'rough' surface

Accurately correlating measured (contact or non-contact method) surface roughness parameters with tactile roughness has proven very difficult (Fujii *et al.* 1997; Fujiwara *et al.* 1998, 2001, 2004). A surface rated very smooth to the touch can have a few very narrow, but deep, fissures caused by slicing along a vessel element that can greatly skew mathematically derived roughness parameters obtained directly from a measured profile. An example of this is the 'smooth'- rated surface of guadua strands, whereby there

is a deep valley caused by slicing lengthways though a vessel element within a fiber bundle (Fig. 2a and Fig. 3a). Topographic features as this had an upwards skew effect on the R_a for 'smooth' guadua strands compared with 'smooth' moso strands, both of which felt similar to the touch. Better linkage of tactile roughness with measured roughness indices is possible using a Robust Gaussian Regression Filter (RFRF) (Brinkmann *et al.* 2000). This reduces or eliminates 'outlier' effects that cannot be discerned by, or affect, the feel of the overall surface (Fujiwara *et al.* 2004). However, if considering surface roughness in relation to adhesion, such filters can mask the presence of topographic features that strongly influence adhesive interaction with the surface and the ability to form adequate bonds.

The results from the surface roughness measurements has potential implications for the efficiency of bonding with small resin droplets dispensed from spinning disk atomizers during OSB strand blending. Numerous studies have shown that for a given dose of resin, many very small droplets or particles of solid resin and wax lead to superior flake or OSB board properties rather than fewer, larger resin spots (Schwarz *et al.* 1968; Kasper and Chow 1980; Ellis 1993; Kamke *et al.* 1996; Saunders and Kamke 1996; Smith 2003 a,b). The size and spacing of the droplets is critical. Optimum resin spot diameter has been shown to be between about 300 μm and 400 μm, with spacing no greater than 300 μm (Smith 2003b). There is no information directly linking the size of the pits and fissures in machined OSB strands with the size of the droplets administered during blending of strands with resin. A recommended droplet diameter for a typical PF resin used in OSB manufacture, dispensed from a spinning disk atomizer (SDA) is 94 μm (Smith 2003b). Experiments using industrial blender operating parameters (resin flow rate, SDA disk rotational speed) by Zhang *et al.* (2008) found much smaller droplet diameters ranging from 0.25 to 60 μm. 90% of the spray volume consisted of droplets <30 μm, and up to 15% of the spray volume consisted of droplets <10 μm in diameter. This was smaller than the average peak-valley difference (R_a), and certainly smaller than the average maximum roughness (R_z) of the rough-surface bamboo strands. If the strands being blended have high peaks and deep valleys, then the very small droplets administered by SDA during blending are likely to disappear into fissures, and will be unable to contribute to bonding. A deeply fissured surface (such as the loose side of a veneer) also creates the opportunity for adhesive over-penetration and starvation of the glueline, particularly for resins with low surface tension (Shupe *et al.* 1998). Therefore, surface roughness and topography of wood adherends, such as veneer or strands, could greatly affect the bond strength depending on the adhesive system, and its amount and distribution on adherends.

The bond strength of discrete and scattered resin spots between OSB strands relies on the ability of strands to plasticize and deform sufficiently during hot pressing to form very tight, continuous wood-wood contact (Wolcott *et al.* 1990). The vast majority of bonds between strands result from a resin spot on one strand contacting a resin-free area on an adjacent strand (Smith 2003b). If smooth, intimate contact between the two surfaces is not made, then a bond is unlikely to be formed, and that resin is wasted. Aspen strands soften, compress and conform tightly to one-another during hot pressing, and administering very small droplets during blending does not appear to pose any significant problems for product quality. Investigations on pressing bamboo strand boards (Semple *et al.* 2015b) found that, unlike aspen, the harder and denser bamboo strands do not compress and conform to each other under normal OSB hot pressing conditions, leaving visible gaps between strands. This means that bonding by tiny, discrete droplets in bamboo strand boards could be more sensitive to the surface roughness of bamboo strands. Further work

bioresources.com

is required to examine the interactions between bond strength formation and the surface roughness of bamboo strands.

CONCLUSIONS

1. Moso and guadua bamboo produced different strand surface quality when stranded using a disk flaker designed for relatively soft, low density woods such as aspen. The majority of guadua strands were visually and tactilely classified as 'rough' on both sides, and only 5% could be considered 'smooth' on both sides. The remainder had one 'rough' and one 'smooth' surface. About a quarter of moso strands were 'smooth' on both sides, compared with 60% of aspen mill strands.

2. Average measured surface roughness (R_a) of the 'smooth' moso strand surface was 7.7 µm, while that of aspen mill strands and guadua were similar at 10.1 µm and 10.7 µm, respectively. The R_a value of 'rough' strand surfaces was 17.4 µm, 20.9 µm, and 23.4 µm for aspen, moso, and guadua, respectively.

3. The average maximum roughness (average distance between the five largest peaks and valleys, Rz) values were similar for all three strand types classified as 'rough'; approximately 115 µm.

4. The average and maximum roughness values for the strand surfaces exceeded the reported diameter of most droplets dispensed by spinning disk atomizers used in OSB furnish blending. This could potentially affect bonding efficiency, particularly in the case of the bamboo strands, in which there was a much greater proportion of very rough strands, and which do not conform and compress during hot pressing.

5. To improve the surface quality of strands from bamboo culms, reduction or elimination of the counter knife profiling, hardened steel blades and frequent knife sharpening and perhaps a reduction in the cutting speed are recommended

ACKNOWLEDGEMENTS

REFERENCES CITED

Aijazi, A. N. (2013). "Material characterization of guadua bamboo and the environmental feasibility of structural bamboo products," B.Sc. Thesis, MIT, Cambridge, MA. pp. 63.

Amada, S., Ichikawa, Y., Munekata, T., Nagase, Y., and Shizu, Y. (1997). "Fiber texture and mechanical graded structure of bamboo," *Compos. B* (28), 13-20. DOI: 10.1016/S1359-8368(01)00022-1.

bioresources.com

Brinkmann, S., Bodschwinna, H., and Lemke, H. W. (2000). "Accessing roughness in three-dimensions using Gaussian regression filter," In: *Proc. 8th International Conference on Metrology and Properties of Engineering Surfaces*, 26-29, April 2000, Huddersfield, UK.

Collett, B. M. (1972). "A review of surface and interfacial adhesion in wood science and related fields," *Wood Sci. Tech.* 6, 1-42. DOI: 10.1007/BF00351806.

Dagilis, T. D. (1999). "Bamboo composite materials for low cost housing," Ph.D. Thesis, Department of Civil Engineering, Queens University, Kingston, ON, 248 pp.

De Vallance, D. B., Gray, J. D., and Grushecky, S. T. (2012). "Improving strand quality of upland oaks for use in oriented strand board," in: *Proc. 18th Central Hardwoods Forest Conference*, 26-28 March 2012, West Virginia University, Morgantown, WV, pp. 284-291.

De Voe, D., Knox, L., and Zhang, G. (1992). "An experimental study of surface roughness assessment using image processing," *University of Maryland Technical Research Report TR 92-28*, 13 pp.

De Vos, V. (2010). "Bamboo for exterior joinery: A research in material properties and market perspectives," B.Sc. Thesis, University of Applied Sciences, Van Hall Larenstein (Wageningen UR), 82 pp.

Dixon, P. G., and Gibson, L. J. (2014). "The structural and mechanics of moso bamboo material," *J. R. Soc. Interface* 11, 20140321. DOI: 10.1098/rsif.2014.0321.

Ebewele, R. O., River, B. H., and Koutsky, J. A. (1980). "Tapered double cantilever beam fracture tests of phenolic-wood adhesive joints Part II: Effects of surface roughness, the nature of surface roughness, and surface aging on joint fracture energy," *Wood Fiber Sci.* 12(1), 40-65.

Ellis, S. (1993). "Effect of resin particle size on waferboard adhesive efficiency," *Wood Fiber Sci.* 25(3), 215-219.

Estrada, M., Linero, D., and Takeuchi, C. (2014). "Variation in the fiber percentage of laminated bamboo specimens," in: *Proc. 15th NOCMAT 2014*, November 23-25 2014, Sao Paulo, Brazil, p. 130.

Fujii, Y., Yoshizane, M., and Okumura, S. (1997). "Evaluation of surface roughness by various parameters I. Relationships between several roughness parameters and tactile roughness (in Japanese)," *Mokuzai Gakkaishi* 43, 574-579.

Fujiwara, Y., Inui, K., Fujii, Y., Sawada, Y., and Okumura, S. (1998). "An approach to the three-dimensional evaluation of the surface roughness of wood: Relationship between the distribution of peaks on the surface and tactile roughness (in Japanese)," *Mokuzai Gakkaishi* 44, 447–451.

Fujiwara, Y., Fujii, Y., Sawada, Y., and Okumura, S. (2001). "Development of a parameter to reflect the roughness of a wood surface that corresponds to tactile roughness: a novel filter to exclude local valley effects," *Holz Roh Werkst.* 59(5), 351–355. DOI: 10.1007/s001070000161.

Fujiwara, Y., Fujii, Y., Sawada, Y., and Okumura, S. (2004). "Assessment of wood surface roughness: Comparison of tactile roughness and three-dimensional parameters derived using a robust Gaussian regression filter," *J. Wood Sci.* 50(1), 35-40. DOI: 10.1007/s10086-003-0529-7.

Grosser, D., and Liese, W. (1971). "On the anatomy of Asian bamboos, with special reference to their vascular bundles," *Wood Sci. Tech.* 5(4), 290-312. DOI: 10.1007/BF00365061.

Hu, C. and Afzal, M. T. (2005). "Automatic measurement of wood surface roughness by laser imaging. Part I: Development of laser imaging system," *Forest Prod. J.* 55(12), 158-163.

ISO 4287 (2000). "Geometrical Product Specifications (GPS) – Surface texture: Profile method – Terms, definitions, and surface texture parameters," International Organization for Standardization, Geneva.

ISO 16610 part 21 (2011). "Geometrical product specifications (GPS) - Filtration - Part 21: Linear profile filters: Gaussian filters," International Organization for Standardization, Geneva.

Kamke, F. A., Lenth, C. A., and Saunders, H. G. (1996). "Measurement of resin and wax distribution on wood flakes," *Forest Prod. J.* 46(6), 63-68.

Kasper, J. B. and Chow, S. (1980). "Determination of resin distribution in flakeboard using x-ray spectrometry," *Forest Prod. J.* 30(7), 37-40.

Leise, W. (1998). "The anatomy of bamboo culms," *INBAR Technical Report 18*, International Network for Bamboo and Rattan, Beijing, pp. 175-191.

Liese, W., and Grosser, D. (1972). "On the variability of fiber length of bamboo," *Holzforschung* 26(6), 202-211. DOI: 10.1515/hfsg.1972.26.6.202.

Liese, W., and Wiener, G. (1996). "Ageing of bamboo culms. A review," *Wood Sci. Tech.* 30(12), 77-89. DOI: 10.1007/BF00224958.

Lundberg, I. A. S., and Porankiewicz, B. (1995). "Studies of non-contact methods for roughness measurements on wood surfaces," *Holz Roh Werkst.* 53(5), 309-314. DOI: 10.1007/s001070050097.

Maldas, D. C., and Kamdem, D. P. (1999). "Wettability of extracted southern pine," *Forest Prod. J.* 49(11/12), 91-93.

Marian, J. E., Stumbo, D. A., and Maxey, C. W. (1958). "Surface texture of wood as related to glue joint strength," *Forest Prod. J.* 8(12), 345-351.

Maietta, A., Dexter, J., and House, T. (2011). "Ring flaker knife assembly and method of use," US Patent 7938155 B2, 20 pp.

Nussbaum, R. M., and Sterley, M. (2002). "The effect of wood extractive content on glue adhesion and surface wettability of wood," *Wood Fiber Sci.* 34(1), 57-71.

Osorio, L., Trujillo, E., Lens, F., Ivens, J., Van Vuure, A., and Verpoest, I. (2010). "The relation between bamboo fiber microstructure and mechanical properties," in: *Proc. 14th European Conference on Composite materials*, 7-10 June 2010, Budapest, Hungary.

Ramirez, F., Gonzalez, M., Maldonado, A., and Nivia, J. (2012). "Bamboo-guadua fibers for composites," in: *Proc. 15th European Conference on Composite Materials*, 24-28 June 2012, Venice, Italy, 15 pp.

Sandak, J., and Tanaka, C. (2003). "Evaluation of surface smoothness by laser displacement sensor I: Effect of wood species," *J. Wood Sci.* 49(4), 305-311. DOI: 10.1007/s10086-002-0486-6.

Sandak, J., Tanaka C., and Ohtani, T. (2004). "Evaluation of surface smoothness by laser displacement sensor II: Comparison of lateral effect photodiode and multi-element diode," *J. Wood Sci.* 50(1), 22-27. DOI: 10.1007/s10086-003-0523-0.

Semple, K. E., Smola, M., Hoffman, J., and Smith, G. D. (2014). "Optimising the stranding of moso bamboo (*Phyllostachys pubescens* Mazel) culms using a CAE 6/36 disk flaker," In: *Proc. 57th International Convention of Society of Wood Science and Technology*, June 23-27, 2014, Zvolen, Slovakia, pp. 257-269.

Semple, K. E., Zhang, P. K., and Smith, G. D. (2015a). "Comparison of stranding and strand quality of two giant timber bamboo species; moso (*Phyllostachys pubescens* Mazel) and guadua (*guadua angustifolia* Kunth) from a CAE 6/36 disk flaker. Part I Tissue characterization, strand production and size classification," *BioResources* 10(3), 4048-4064. DOI: 10.15376/biores.10.3.4048-4064.

Semple, K. E., Zhang, P. K., and Smith, G. D. (2015b). "Hybrid oriented strand boards made from Moso bamboo (*Phyllostachys pubescens* Mazel) and Aspen (*Populus tremuloides* Michx.): Species-separated three-layer boards," *Eur. J. Wood Prod.* (online): DOI 10.1007/s00107-015-0914-0.

Saunders, H. G., and Kamke, F. A. (1996). "Quantifying emulsified wax distribution on wood flakes," *Forest Prod. J.* 46(3), 56-62.

Schwarz, F. E., Andersen, R. L., and Kageler, A. G. (1968). "Resin distribution and how variation affects board quality," In: *Proc. 2nd Symposium on Particleboard*, 27-29 March, 1968, Washing State University, Pullman, Washington.

Shao, Z. P., Zhou, L., Liu, Y. M., Wu, X. M., and Arnaud, C. (2010). "Differences in structure and strength between internode and node sections of moso bamboo," *J. Trop. For. Sci.* 22(2), 133-138.

Shi, S. Q., and Gardner, J. (2001). "Dynamic adhesive wettability of wood," *Wood Fiber Sci.* 33(1), 58-68.

Smith, G. D. (2003a). "A laboratory technique for coating strands with resin droplets of controlled size and spacing," *Forest Prod. J.* 53(7/8), 70-76.

Smith, G. D. (2003b). "The lap shear strength of droplets arrays of a PF-resin on OSB strands," *Forest Prod. J.* 53(11/12), 67-73.

Shupe, T. E., Hse, C.Y., Choong, E. T., and Groom, L. H. (1998). "Effect of wood grain and veneer side on loblolly pine veneer wettability," *Forest Prod. J.* 48(6), 95-97.

Spelter, H. (1991). "Recent developments in veneer peeling confront quality variables," *Panel World* 5(May 1991), 54-65.

Trujillo, E., Osorio, L., Van Vuure, A.W., Ivens, J., and Verpoest I. (2010). "Characterization of polymer composite materials based on bamboo fibers," in: *Proc. 14th European Conference on Composite Materials*, 7-10 June 2010, Budapest, Hungary, 10 pp.

Van Vuure, A. W., Osario, L., Trujillo, E., Fuentes, C., and Verpoest, I. (2009). "Long bamboo fiber composites," in: *Proc. 18th International Conference on Composite Materials*, 27-31 July 2009, Edinburgh, Scotland, 5 pp.

Wolcott, M. P., Kamke, F. A., and Dillard, D. A. (1990). "Fundamentals of flakeboard manufacture: Viscoelastic behavior of the wood component," *Wood Fiber Sci.* 22(4), 345-361.

Zhang, X., Muszyinski, L., and Gardner, D. J. (2008). "Spinning atomization of wood resin-adhesives: I. Spray characteristics, atomization mechanism, and resin efficiency," *Forest Prod. J.* 58(11), 62-68.